ALEPH 93-161
PHYSIC 93-138
A. Halley and P. Colrain
7.10.1993

A Measurement of the b Quark Hemisphere Charge Using a Lifetime-Tag in the 1992 Data

Andrew Halley (Max-Planck-Institut für Physik, München)
Paul Colrain (The University of Glasgow, Scotland)

6^{th} October 1993

Abstract

This note describes a measurement of the hemisphere charge of b quarks in ALEPH when using the weighted charge summation, or jet-charge, technique. The measurement is performed using the moments of the two hemisphere charges in events selected using the lifetime-tag algorithm QIPBTAG.

1 Motivation

Techniques which make use of quark charge retention in jets have been widely used recently for both Electroweak [1, 2, 3] and Mixing [4] measurements. These rely upon Monte Carlo models to predict the fraction of the parent quark's charge which is retained by its fragmented jet. More recently, it has been shown that measurements of quark-signed hemisphere charges in data can be used to severely constrain the systematic uncertainties in these measurements by limiting their dependence on fragmentation models [5, 6]. This is the purpose of measuring the b-quark's mean hemisphere charge, δ_b, in ALEPH data.

Previously δ_b has been measured in the b system using high (p, p_t) leptons to tag both the charge and type of quark present in the sample [4, 7].The current measurement describes an alternative technique which makes use of the opposite signs of the quark charges in either hemisphere of hadronic events. A lifetime-tag is used to select an enriched sample of b quarks in order to measure the b hemisphere-charge. This measurement makes equal use of both hemispheres in an event, and hence automatically incorporates the "correct" $B^0 - \bar{B}^0$ mixing fraction. In this sense, the mixing is seen simply as further diluting the fraction of the b quark's charge retained by its fragmented jet.

The methods described in this document are generally applicable to any sample of hadronic events where both hemispheres are unbiased. Knowledge of δ_b from data also opens the door to future mixing measurements using the hemisphere charge instead of di-leptons.

2 Useful Relations

It is useful to recall some definitions and the terminology of hemisphere-charge measurements to clarify the following discussion. Assuming hadronic $Z \rightarrow f\bar{f}$ production, the charges of hemispheres separated by the thrust axis are defined using a weighted charge summation as described in [1, 2, 4]. These are labelled Q_F and Q_B, depending on whether the hemisphere is predominately in the *forward* (+Z) or *backward* (-Z) half of the detector. The following quantities are then defined :

The *Charge Difference*	$\equiv Q_{FB}$	$= Q_F - Q_B$	with width, σ_{FB}, and
The *Total Charge*	$\equiv Q$	$= Q_F + Q_B$	with width, σ_Q

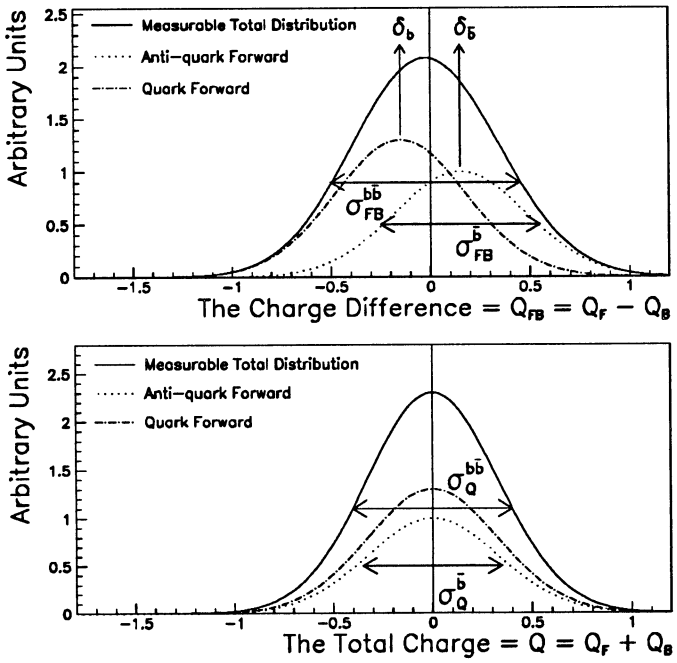

Figure 1: *Schematic illustration of the Q_{FB} and Q charge distributions for the case of b quarks only.*

An example of these distributions is shown in Figure 1 for the case when only b quarks are present. It is then possible to define :

$$\bar{\delta}^2 = (\sigma_{FB})^2 - (\sigma_Q)^2 \tag{1}$$

which approximates the square of the *mean hemisphere-charge separation*, $\langle \delta_f \rangle$. This may be understood by noting that Q_{FB} contains roughly twice the amount of retained quark charge in a hemisphere whilst in Q this effectively cancels, apart from the uncertainty in the charge measurement itself. Relation (1) may be considered then simply as subtracting the effective *charge resolution* ($\sigma_Q^{f\bar{f}}$) in quadrature from the broadened Q_{FB} distribution width, $\sigma_{FB}^{f\bar{f}}$. The method employed to extract δ_b is explained in detail in the Appendix and uses the relation :

$$\delta_b^2 = \underbrace{\bar{\delta}_b^2 + \langle Q_{FB}^{b\bar{b}} \rangle^2}_{Measured\ in\ Data} - \underbrace{\left[\left(\sigma_{FB}^b\right)^2 - \left(\sigma_Q^b\right)^2 \right]}_{\text{"Correlation Correction"}} \tag{2}$$

where $\bar{\delta}_b$ is the value of $\bar{\delta}$ if only b quarks were present. $\bar{\delta}_b$ is measured in data by studying the dependence of $\bar{\delta}$ as a function of b-purity. The value of $\langle Q_{FB}^{b\bar{b}} \rangle$ is taken from the lifetime-tagged $A_{FB}^{b\bar{b}}$ analysis [8] whereas the correlation corrections are obtained from simulated, Monte Carlo events. Both the correlation corrections and $\langle Q_{FB}^{b\bar{b}} \rangle^2$ are small compared to the measured $\bar{\delta}_b$.

3 Experimental Method

The relations described above are most easily applied to a sample of events containing a single flavour of quark. In practice this is difficult to achieve with sufficient statistical precision. The method employed here makes use of the available data of all flavours to *extrapolate* measured quantities to the case of 100% b-purity. This method relies only on a smooth dependence of $\bar{\delta}$ on the b-purity of the event sample. The expected contributions to $\bar{\delta}$, shown in Figure 2,

indicate that this is indeed the case. The method used to extract δ_b from data may be then briefly summarised as follows :

- Selection of hadronic events and assignment of the thrust axis.
- Application of the lifetime-tagging algorithm to select heavy flavour events.
- Calculation of the hemisphere charges for a range of values of weighting power, κ.
- Evaluation of $\bar{\delta}$ using relation (1) for events passing successively more stringent cuts on the lifetime-tag probabilities. This has the effect of producing a purer and purer b sample.
- The variation of $\bar{\delta}$ with b purity, $\mathcal{P}_b$, is then used to extrapolate to the limiting case of 100% b purity where $\bar{\delta} \rightarrow \bar{\delta}_b$.

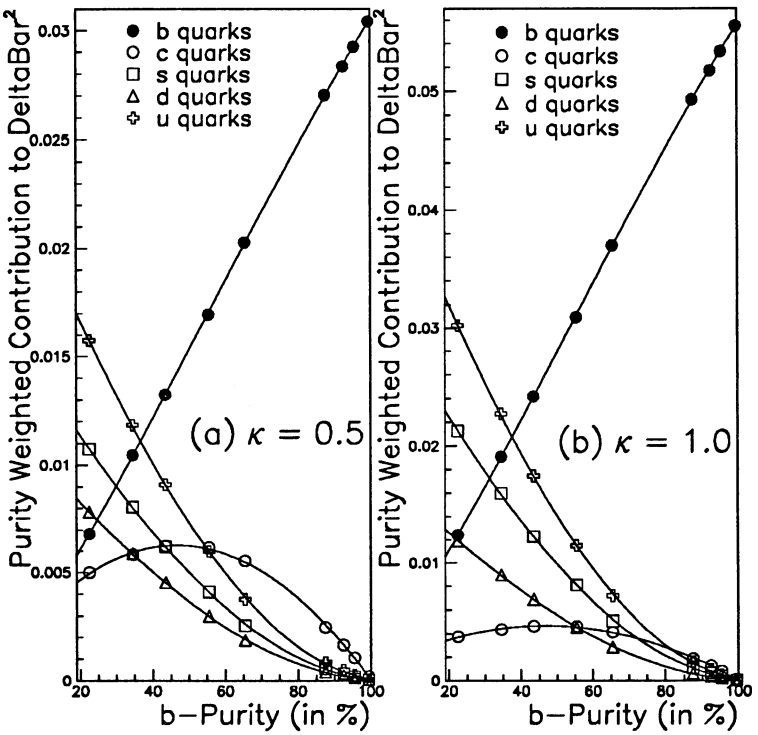

Figure 2: *Expected contributions to $\bar{\delta}$ from the various quark flavours in simulated Monte Carlo events for κ values of 0.5 and 1.0. Note the persistent c-quark background contribution at high b-purities and lower κ values.*

The extrapolated values of $\bar{\delta}_b$ in data are corrected for the correlations between charge-finding in the two hemispheres. The relatively small *correlation corrections* of equation (2) are derived from a large sample of fully simulated Monte Carlo events and used to extract δ_b. It is important to note that Monte Carlo is only used at the level of a correction to the $\bar{\delta}_b$ measurements in data. The following sections describe the experimental procedure in more detail.

3.1 Event Selection and Tagging

Events are selected for the analysis using VDET selected runs from 1992 with SCANBOOK. No preselection is made based on the tracking quality of the 1992 data. Hadronic events are then selected using the $q\bar{q}$ charged track event selection (CLAS 16) algorithm. The thrust axis is

determined using **ENFLW** objects after "good" charged tracks have been selected according to the $q\bar{q}$ track criteria. The thrust axis is then constrained to lie within the angular acceptance of $\mid cos\,\theta_{thrust} \mid < 0.8$. An additional 200 MeV/c P_T cut is placed on tracks used for the hemisphere charge calculations.

The **QIPBTAG**, lifetime-tag, algorithm [9] is applied, and the two *hemisphere tag probabilties* for each event are calculated. An increasingly pure b sample is obtained by demanding that *at least one* hemisphere passes a given cut on these hemisphere tag probabilties. It is then useful to define :

$$\begin{aligned} \varepsilon_f^h &= \text{the efficiency to tag a hemisphere of flavour } f, \\ \varepsilon_f^e &= \text{the efficiency to tag an event of flavour } f, \end{aligned} \tag{3}$$

which are related by :

$$\varepsilon_f^e = 2\varepsilon_f^h\left(1 - c_f\varepsilon_f^h\right) + c_f\left(\varepsilon_f^h\right)^2. \tag{4}$$

c_f are the flavour-dependent correlations between the hemispheres, of which only the b term, c_b, is of significance. These correlation terms may be related to the λ_f of the $\Gamma_{b\bar{b}}$ analysis [9] via the relation :

$$c_f = \lambda_f \frac{1}{\varepsilon_f^h}\left(1 - \varepsilon_f^h\right) + 1 \tag{5}$$

The values for ε_f^h and λ_f are those used[1] in the ALEPH $\Gamma_{b\bar{b}}$ analysis [10]. To ensure an accurate extrapolation through the full range of b purities, a set of 9 hemisphere tag cuts are used in the range from $-log_{10}(tag\ cut) = 0.1 \rightarrow 5.9$. The purities for different flavours are then calculated using :

$$\mathcal{P}_f = \frac{\varepsilon_f^e}{\varepsilon_{Total}^e}\frac{\Gamma_{f\bar{f}}}{\Gamma_{had}} \tag{6}$$

where ε_{Total}^e is the overall tagging efficiency for all flavours combined.

The values for $\Gamma_{c\bar{c}}$ and $\Gamma_{b\bar{b}}$ are correlated with the values of ε_f^h and ε_f^e. The expected Standard Model (SM) values are assumed for light quarks as their significance is small. They are then re-scaled so that the total of the light quark fractions, and $(\Gamma_{c\bar{c}}, \Gamma_{b\bar{b}})$ from [10], is unity. These values are summarised in Table 1. The resulting purities for these tag cuts are shown in Table 2.

$-log_{10}(cut)$	$\Gamma_{u\bar{u}}/\Gamma_{had}$	$\Gamma_{d\bar{d}}/\Gamma_{had}$	$\Gamma_{s\bar{s}}/\Gamma_{had}$	$\Gamma_{c\bar{c}}/\Gamma_{had}$	$\Gamma_{b\bar{b}}/\Gamma_{had}$
0.1	0.1707	0.2191	0.2191	0.1710	0.2094
0.6	0.1741	0.2234	0.2234	0.1710	0.2214
0.9	0.1739	0.2232	0.2232	0.1710	0.2210
1.3	0.1734	0.2225	0.2225	0.1710	0.2191
1.7	0.1732	0.2223	0.2223	0.1710	0.2184
3.0	0.1729	0.2219	0.2219	0.1710	0.2174
3.5	0.1735	0.2227	0.2227	0.1710	0.2195
4.0	0.1733	0.2224	0.2224	0.1710	0.2187
5.9	0.1743	0.2236	0.2236	0.1710	0.2221

Table 1: *Quark fractions used to calculate the sample flavour purities.*

The errors on the purities fully take into account those from [10].

[1]The author is very grateful to Dave Brown (MPI Muenchen) for the use of these numbers.

$-log_{10}(cut)$	$\mathcal{P}_u$	$\mathcal{P}_d$	$\mathcal{P}_s$	$\mathcal{P}_c$	$\mathcal{P}_b$
0.1	16.8(±0.2)	21.6(±0.2)	21.6(±0.2)	17.8(±0.1)	22.2(±0.2)
0.6	12.7(±0.3)	16.2(±0.4)	16.2(±0.4)	20.8(±0.3)	34.1(±0.6)
0.9	9.7 (±0.4)	12.5(±0.5)	12.5(±0.5)	22.2(±0.4)	43.1(±0.9)
1.3	6.4 (±0.4)	8.2 (±0.6)	8.2(±0.6)	22.0(±0.6)	55.2(±1.2)
1.7	4.0 (±0.5)	5.2 (±0.6)	5.2(±0.6)	19.7(±0.8)	65.0(±1.4)
3.0	0.9 (±0.3)	1.2 (±0.4)	1.2(±0.4)	8.8(±0.7)	88.0(±1.4)
3.5	0.5 (±0.2)	0.8 (±0.3)	0.8(±0.3)	5.9(±0.7)	92.3(±1.3)
4.0	0.3 (±0.1)	0.4 (±0.2)	0.4(±0.2)	3.8(±0.6)	95.2(±1.3)
5.9	0.0 (±0.2)	0.1 (±0.3)	0.1(±0.3)	0.7(±0.4)	99.0(±3.1)

Table 2: *Purities of the quark flavours making up the samples of events used.*

3.2 Charge Determination and $\bar{\delta}$ Measurement

The hemisphere charges, Q_F and Q_B, are measured for each event using the weighted charge summation of [1] and a range of κ values. The widths of the Q_{FB} and Q distributions are measured in subsamples of events passing the lifetime-tag cuts described in Section 3.1. These are then used to calculate the values of $\bar{\delta}$. For example, at $\kappa = 0.5$ these are shown in Table 3. The downward trend of $\bar{\delta}(\mathcal{P}_b)$ is apparent and is shown in Figure 3. This can be understood from

b Quark Purity	*Raw $\bar{\delta}$ Values*
22.2 (± 0.2) %	0.2180 (± 0.0012)
34.1 (± 0.6) %	0.2071 (± 0.0009)
43.1 (± 0.9) %	0.1992 (± 0.0008)
55.2 (± 1.2) %	0.1902 (± 0.0010)
65.0 (± 1.4) %	0.1815 (± 0.0011)
88.0 (± 1.4) %	0.1679 (± 0.0022)
92.3 (± 1.3) %	0.1650 (± 0.0016)
95.2 (± 1.3) %	0.1623 (± 0.0017)
99.0 (± 3.1) %	0.1503 (± 0.0048)

Table 3: *The raw values of $\bar{\delta}$, for $\kappa = 0.5$, in subsamples of events selected with increasing b purity.*

the behaviour shown in Figure 2, and by considering that :

$$\bar{\delta} \equiv \bar{\delta}_{f\bar{f}} = \sqrt{\sum_{f=u,d...}^{b} \bar{\delta}_f^2 \frac{\Gamma_{f\bar{f}}}{\Gamma_{had}} \frac{\varepsilon_f^e}{\varepsilon_{Total}^e}} \tag{7}$$

u-quarks have the largest values of $\bar{\delta}_f$ and so, in an untagged hadronic sample, the large contribution from the (u, d, s) values of $\bar{\delta}_f$ is expected to dominate the *mean* measured value. However, as the b purity increases, the light quark flavours are quickly suppressed and the main contamination is from c quarks. These have the smallest value for $\bar{\delta}_f$ of all the quarks. Hence the reduction in the gradient of $\bar{\delta}$ as the lifetime-tag cut increases the fraction of heavy flavours and allows $\bar{\delta}$ to tend towards its asymptotic value, $\bar{\delta}_b$.

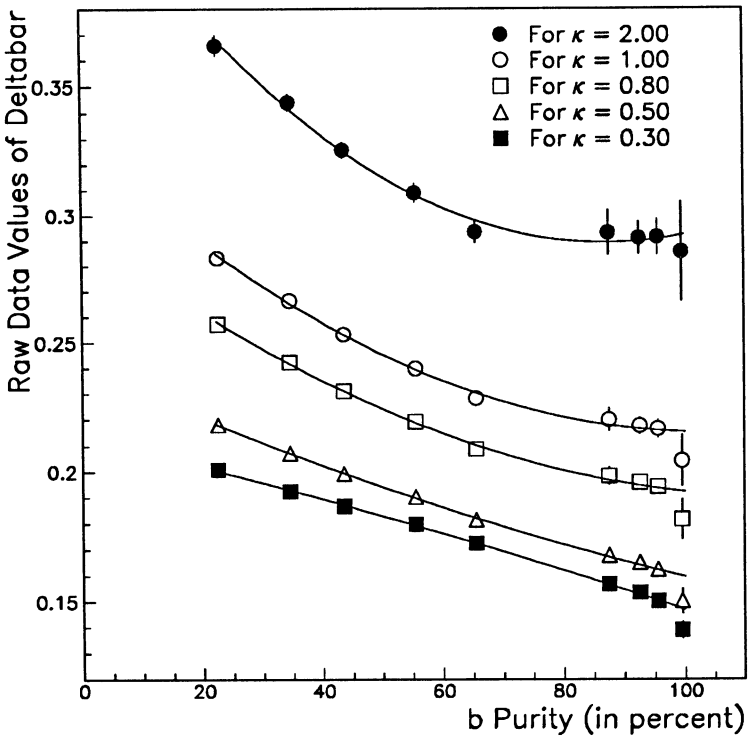

Figure 3: *The variation of the raw $\bar{\delta}$ values in data as a function the b purity of the event subsample. Lines are drawn to guide the eye.*

3.3 The Lifetime Dependence of $\bar{\delta}$

The QIPBTAG algorithm is used to preferentially select events with a large, visible "lifetime". It combines track impact-parameter information in the hemispheres of an event to return a probabilty that this hemisphere arises from (u, d, s) quark production [9]. Table 4 indicates that there is a slight increase in the number of charged tracks and their mean momentum for events passing the more stringent lifetime-tag cuts. It is important to study and correct for any bias

Lifetime Tag Hemisphere Cut	*Selected Charged Track Multiplicity*	*Mean Charged Track Momentum*
1.0000	20.40 (± 0.01)	2.676 (± 0.002)
0.0500	20.67 (± 0.01)	2.720 (± 0.002)
0.0100	20.77 (± 0.01)	2.738 (± 0.002)
0.0050	20.81 (± 0.01)	2.744 (± 0.002)
0.0010	20.91 (± 0.01)	2.756 (± 0.002)
0.0005	20.96 (± 0.01)	2.760 (± 0.002)
0.0001	21.09 (± 0.02)	2.764 (± 0.003)

Table 4: *Mean number and momentum of charged tracks selected by the $q\bar{q}$ selection criteria for simulated b events surviving increasingly stringent lifetime-tag cuts.*

this may cause to the hemisphere charge determination.

It is rather delicate to isolate such effects since the quark flavours in the sample alter with the lifetime-tag cut, as do the characteristics of the hemisphere charges. However, it is possible to make use of tagged and untagged hemispheres *in the same event* to do this. This is performed

by comparing the widths of charge distributions from hemispheres in events where only one hemisphere passes the tag, and the other does not. The study is then performed for a series of lifetime-tag cuts. At each cut, the flavour composition of the tagged and untagged hemisphere charges is the same. The results are shown in Figure 4 (a) and (c). These distributions show

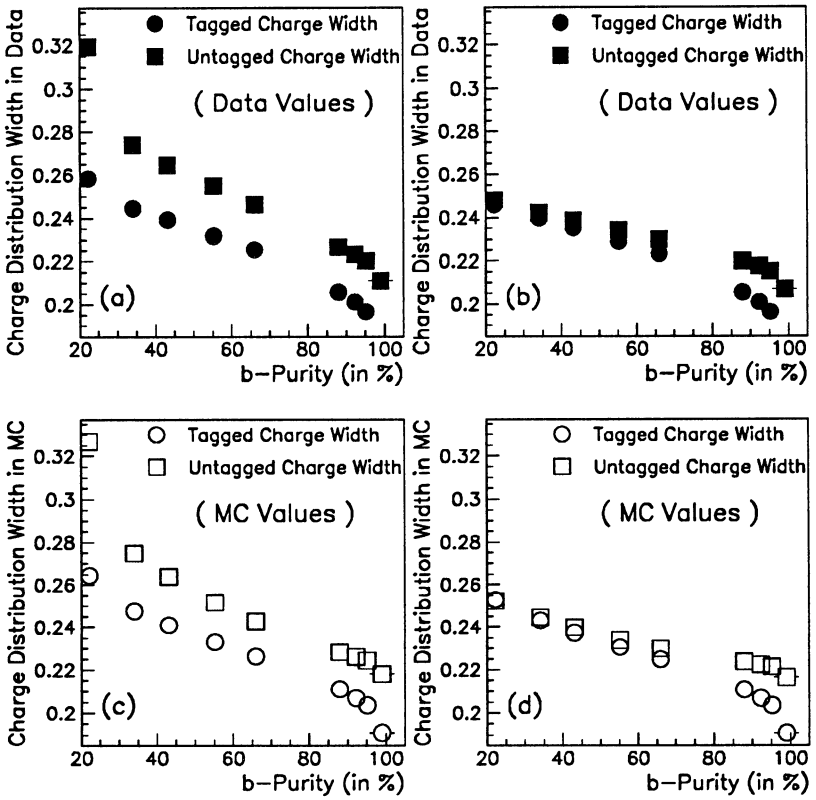

Figure 4: *Widths of the hemisphere charge distributions for tagged and untagged hemispheres. (a) and (c) show the trends in data and simulated events without any conditions. (b) and (d) show the cases with the condition that untagged hemispheres have at least one track passing the* `QIPBTAG` *track selection criteria.*

that tagged hemispheres consistently have a slightly narrower charge distribution than untagged hemispheres.

Figure 4 also shows the widths of the charge distributions after requiring that, for untagged hemispheres, there has to be at least one high-quality track passing the `QIPBTAG` criteria which *would have allowed* it to tag *if* it posessed a sufficiently large impact-parameter. The corresponding data and Monte Carlo trends are shown in Figure 4 (b) and (d). These indicate that making this requirement substantially reduces the differences between tagged and untagged hemispheres at low purities. The difference between tagged and untagged widths manifests itself again at high purities where many such high-quality tracks are required. This strongly suggests that the effect has its source in the slightly different kinematics of tagged hemispheres.

The ratio of the tagged to untagged charge distribution widths is shown in Figure 5 for data and Monte Carlo. The Monte Carlo points in Figure 4 reproduce the trends observed in data, both with and without the condition of "taggable" tracks in untagged hemispheres. The agreement between data and Monte Carlo in the prediction of such trends rules out the possibility that they may be due to the lifetime-tag preferentially selecting different B decay modes. In the `HVFLO3` production used, all B lifetimes are set to the same value.

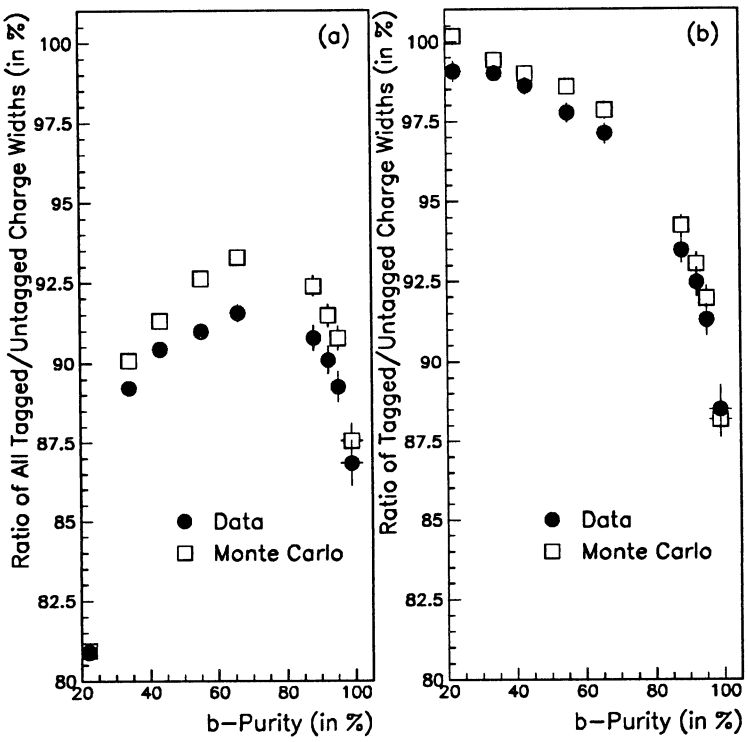

Figure 5: *Ratio of the width of the hemisphere charge distributions for; (a) tagged and untagged hemispheres and; (b) given the condition that untagged hemispheres have at least one track passing the* QIPBTAG *track selection criteria.*

3.4 Lifetime Dependent Corrections to $\bar{\delta}$

If the fit of $\bar{\delta}$ versus b-purity is to remain unbiased, the lifetime-dependent effects described above must be corrected for.

Given that the effects are small, and well modelled by the Monte Carlo, the lifetime dependence of simulated $\bar{\delta}_f$'s are used to correct the raw $\bar{\delta}$ data values. The corrections to the raw $\bar{\delta}$ values in data are calculated using :

$$Correction = \bar{\delta}_{MC}^{tagged} - \bar{\delta}_{MC}^{untagged} == \sqrt{\sum_{f=u,d...}^{b} \mathcal{P}_f \left(\bar{\delta}_f^2\right)^{tagged}} - \sqrt{\sum_{f=u,d...}^{b} \mathcal{P}_f \left(\bar{\delta}_f^2\right)^{untagged}} \quad (8)$$

The correction is applied as an absolute shift to $\bar{\delta}(\mathcal{P}_f)$ in data. The statistical errors on the corrections[2] are augmented by a systematic uncertainty taken from the difference between data and Monte Carlo observed in Figure 5. This amounts to an additional 20% relative systematic uncertainty on the corrections.

The corrections, corrected $\bar{\delta}$ data values and errors are given in Table 5 for the case of $\kappa = 0.5$. The corrections, for a range of κ values, are shown in Figure 6 while their effect is demonstrated in Figure 7. The small increase in the extrapolated value of $\bar{\delta}_b$ is apparent.

3.5 Fit of $\bar{\delta}$ Versus b-Purity to Obtain $\bar{\delta}_b$

The purpose of performing a fit to $\bar{\delta}(\mathcal{P}_b)$ is to extract $\bar{\delta}$ at the limit where $\mathcal{P}_b \rightarrow 100\%$. The lifetime-dependence corrected values of $\bar{\delta}$ and the values of $\mathcal{P}_b$ given in Table 5 are used for this

[2]Which become sizeable at high b-purities when the (u, d, s, c) statistics are low.

b Quark Purity	*Lifetime Dependent Corrections*	*Lifetime Corrected $\bar{\delta}$ Values*
22.2 (± 0.2) %	0.00000 (± 0.00000)	0.2180 (± 0.0014)
34.1 (± 0.6) %	0.00184 (± 0.00155)	0.2089 (± 0.0018)
43.1 (± 0.9) %	0.00343 (± 0.00199)	0.2026 (± 0.0023)
55.2 (± 1.2) %	0.00380 (± 0.00247)	0.1940 (± 0.0028)
65.0 (± 1.4) %	0.00295 (± 0.00279)	0.1845 (± 0.0030)
88.0 (± 1.4) %	0.00473 (± 0.00231)	0.1726 (± 0.0033)
92.3 (± 1.3) %	0.00529 (± 0.00195)	0.1703 (± 0.0027)
95.2 (± 1.3) %	0.00669 (± 0.00175)	0.1690 (± 0.0028)
99.0 (± 3.1) %	0.01625 (± 0.00386)	0.1665 (± 0.0070)

Table 5: *The lifetime dependent corrections and corrected values of $\bar{\delta}$, for $\kappa = 0.5$, in subsamples of events selected with increasing b purity.*

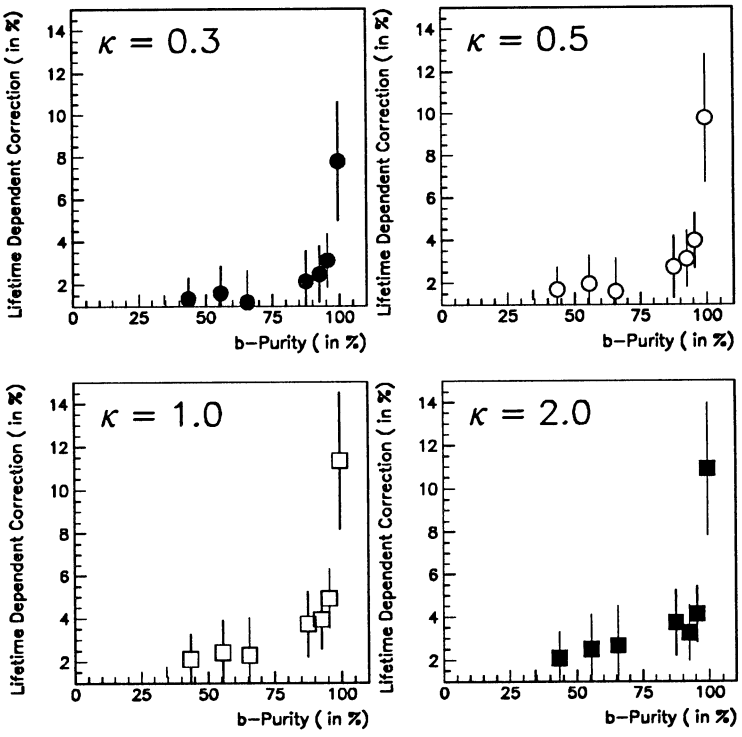

Figure 6: *The lifetime-dependent corrections (in %) to $\bar{\delta}$ for a range of κ values. The errors include contributions from Monte Carlo statistics and the systematic error from the observed difference between data and Monte Carlo charge distribution widths as a function of lifetime.*

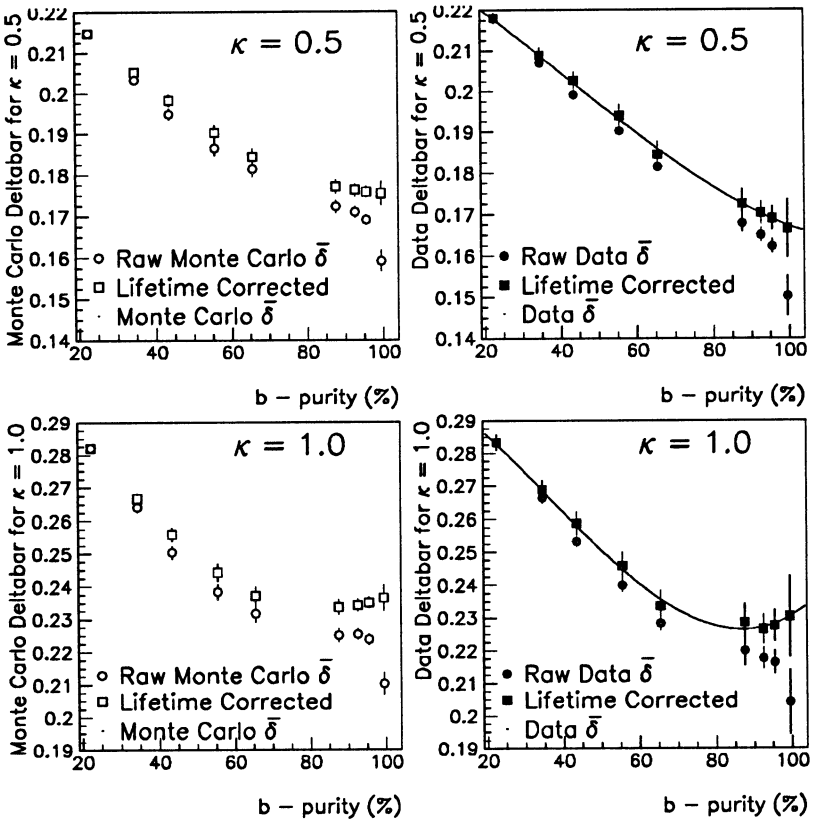

Figure 7: *Illustration of how the lifetime-dependent corrections are applied from Monte Carlo to data for two different κ values. The fitted functions in data are that used to extract $\bar{\delta}_b$.*

purpose. The underlying function of $\bar{\delta}(\mathcal{P}_b)$ is a convolution of the δ_f's and the $\mathcal{P}_f$'s for the 5 quark flavours involved. As such, the form of the fit is essentially empirical in nature. A linear extrapolation is excluded as three types of regime are present. Initially (u, d, s) flavours dominate at low b purities, followed by a "heavy flavour regime" where effectively only (c, b) flavours are present and finally by the case where there is an almost totally pure b-sample. Consequently a cubic polynomial is used to extract $\bar{\delta}_b$. Essentially the background contributions, apparent in Figure 2, exclude a linear extrapolation.

There are correlations between $\bar{\delta}$ measurements at each lifetime-tag cut because the measurement is made in a strict subsample of events passing the previous cut. A full correlation matrix of the data points is used where the statistical correlation coefficients (off-diagonal elements) between points are defined as :

$$Cov\left[\frac{\sum_{i=1}^{n_1} y_i}{n_1}, \frac{\sum_{i=1}^{n_2} y_i}{n_2}\right] = \frac{n_2}{n_1} Cov\left[\frac{\sum_{i=1}^{n_2} y_i}{n_2}, \frac{\sum_{i=1}^{n_2} y_i}{n_2}\right] = \frac{1}{n_1}\sigma_1\,\sigma_2 \tag{9}$$

for the case where $n_1 > n_2$. In this case the σ's must also be scaled to take into account the fact that they are correlated with each other. These are defined as :

$$\sigma_2 = \sigma_1 \sqrt{1 - \frac{n_2}{n_1}} \tag{10}$$

A cubic χ^2 fit is then performed. As the deviations from a straight line are generally small, the second order terms are only loosely constrained. This results in substantial correlations between the three fit parameters. The results of the fits for various κ values are shown in Figure 8. In reality, the correlations between points have little effect on the final result. This is because the

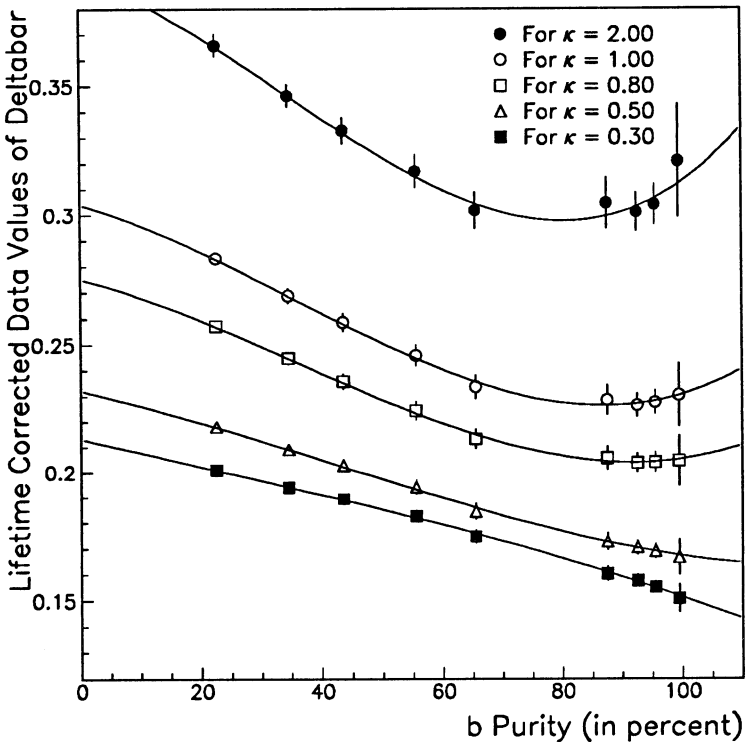

Figure 8: *The variation of the lifetime-corrected $\bar{\delta}$ values in data as a function the b purity of the event subsample.*

QIPBTAG efficiency is a rapidly decreasing function and the data points at lower purities constrain the fit. These effects can be observed in Table 6 where the stability of $\bar{\delta_b}$ under different fitting conditions is shown. From this, it is clear that the intercorrelation between data points has a

Fit Type	*Using Errors*	*Correlated Points*	*Correlated Errors*	*Extracted* $\bar{\delta_b}$	*Error*
Linear	*No*	*No*	*No*	0.1649	(± 0.0012)
Linear	*Yes*	*No*	*No*	0.1640	(± 0.0018)
Linear	*Yes*	*No*	*Yes*	0.1644	(± 0.0016)
Linear	*Yes*	*Yes*	*No*	0.1640	(± 0.0018)
Linear	*Yes*	*Yes*	*Yes*	0.1644	(± 0.0016)
Cubic	*Yes*	*Yes*	*No*	0.1671	(± 0.0045)
Cubic	*Yes*	*No*	*Yes*	0.1672	(± 0.0034)
Cubic	*Yes*	*Yes*	*Yes*	0.1672	(± 0.0034)

Table 6: *Extracted values of $\bar{\delta_b}$ using various fitting procedures to demonstrate the stability of the extrapolation to 100% b-purity at $\kappa = 0.5$.*

very small effect on the fitted value of $\bar{\delta_b}$. The correlated statistical *errors* however, substantially reduce the uncorrelated fit error.

The extracted values of $\bar{\delta_b}$ are given in Table 7 for various κ values.

κ	*Extracted* $\bar{\delta_b}$	*Error*
0.3	0.1513	(± 0.0028)
0.4	0.1577	(± 0.0030)
0.5	0.1672	(± 0.0034)
0.6	0.1791	(± 0.0038)
0.8	0.2050	(± 0.0047)
0.9	0.2178	(± 0.0051)
1.0	0.2307	(± 0.0056)
1.5	0.2813	(± 0.0076)
2.0	0.3127	(± 0.0093)
∞	0.3378	(± 0.0222)

Table 7: *Extracted values of* $\bar{\delta_b}$ *as a function of the weighting parameter* κ.

3.6 Extraction of δ_b from $\bar{\delta_b}$

Equation 2 contains two small correction factors which must be applied to $\bar{\delta_b}$ to obtain δ_b. The first of these, $\langle Q_{FB}^{b\bar{b}} \rangle$, represents the electroweak asymmetry measured in a pure b-sample. These values are measured in data from the the analysis of [8] for the case of a $\sim$ 95% pure b-sample. The values of $\langle Q_{FB}^{b\bar{b}} \rangle^2$ are of order $\sim 10^{-4}$ and are given in Table 8. The $\sim$ 10% uncertainty on the data measurements may be safely neglected.

The *correlation corrections* of equation (2) are taken from the large sample of 1992 mixed $\bar{q}q$ and $\bar{b}b$ events. The correlations are equal for quark and antiquark-forward configurations and so the average of the two is used. These values are given as a function of κ in Table 8. The relatively small effect of these corrections can be seen clearly in Figure 9. The corrections

κ	$\langle Q_{FB}^{b\bar{b}} \rangle^2$	*Correlation Corrections*	δ_b	$\Delta\delta_b$
0.3	0.00008	0.0108 (± 0.0003)	0.1102	0.0040
0.4	0.00013	0.0092 (± 0.0004)	0.1258	0.0040
0.5	0.00016	0.0082 (± 0.0004)	0.1413	0.0043
0.6	0.00019	0.0076 (± 0.0006)	0.1570	0.0046
0.8	0.00026	0.0076 (± 0.0009)	0.1863	0.0055
0.9	0.00029	0.0079 (± 0.0010)	0.1996	0.0060
1.0	0.00032	0.0084 (± 0.0012)	0.2126	0.0065
1.5	0.00046	0.0112 (± 0.0023)	0.2615	0.0089
2.0	0.00045	0.0136 (± 0.0032)	0.2909	0.0109
∞	0.00068	0.0176 (± 0.0099)	0.3118	0.0269

Table 8: *The correlation corrections calculated from Monte Carlo events and applied to* $\bar{\delta_b}$ *in order to extract* δ_b. *The errors on* δ_b *include the statistical uncertainty on the* $\bar{\delta}$ *measurements, that on the lifetime-dependent corrections and the 20% systematic uncertainty on the corrections from the data-Monte Carlo difference.*

are calculated from the quadratic difference between the widths of two closely related charge distributions. This means that they have a large relative error which contributes significantly to the "statistical" error on the δ_b measurement when they are subtracted in quadrature. A improvement is possible by calculating the correlation term :

$$-4\left[\langle Q_F^f Q_B^f \rangle - \langle Q_F^f \rangle \langle Q_B^f \rangle\right] \tag{11}$$

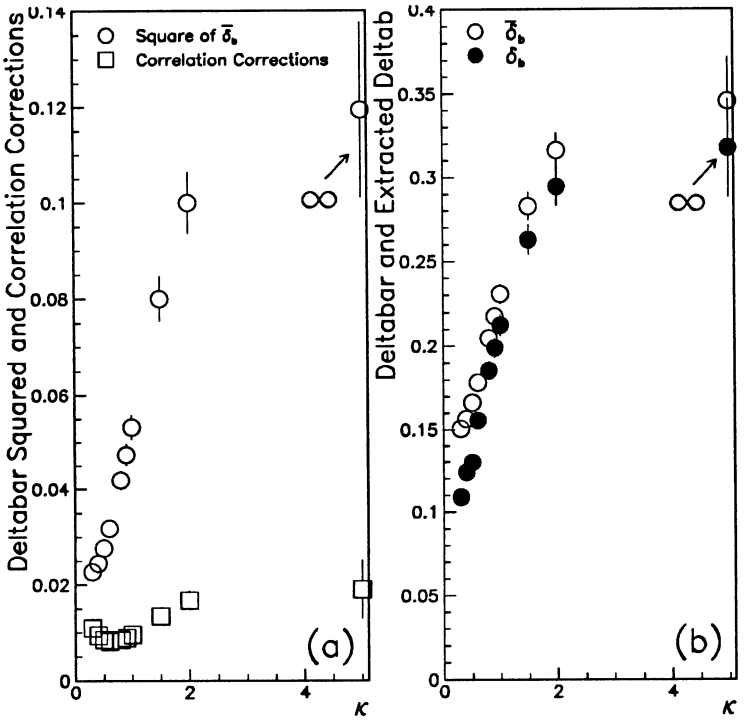

Figure 9: *(a) A comparison of $\bar{\delta}_b^2(\kappa)$ and the charge correlation corrections which are subtracted in quadrature and (b) the effect of applying these corrections to obtain δ_b from $\bar{\delta}_b$.*

as opposed to $\left(\sigma_{FB}^f\right)^2 - \left(\sigma_Q^f\right)^2$ as it can be more accurately extracted.

Applying these correlation corrections to the fitted values of $\bar{\delta}_b$ of Table 7 yields the final values of δ_b given in Table 8.

4 Systematic Uncertainties

There are two significant sources of systematic errors in this measurement :

- Lifetime-Dependent Systematics : These arise from the need to apply the lifetime-dependent corrections to $\bar{\delta}(\mathcal{P}_b)$. These are already included in the fit and so in the extracted $\delta_b(\pm\Delta\delta_b)$ values given in Table 8.

- Correlation Correction Systematics : These arise from the correlation corrections applied to the fitted values of $\bar{\delta}_b$ to obtain δ_b. As these corrections are estimated from Monte Carlo, it is necessary to ensure that they are not dependent upon the parameters of the fragmentation model used. Such systematic uncertainties should have a very small effect on the final result due the relatively small magnitude of the corrections themselves.

The latter of these systematic errors is studied by varying a large number of HVFL03 parameters[3] and observing their effect on the correlation corrections. A large sample of events is generated with the generator's default parameters. For each of the parameters listed in Table 9, event samples are generated at either extremity of the range. As the correlation terms are only applied to the extracted values of $\bar{\delta}_b$ then only those fragmentation parameters relevant to the

[3]This is perfomed at the KINGAL generator level.

Model Parameter	*Lower Extremity*	*Default*	*Upper Extremity*	*Lower Bound of Range*	*Upper Bound of Range*
λ_{QCD}	0.260	0.311	0.400	0.286	0.336
M_{min}	1.600	1.900	2.000	1.740	2.060
σ	0.340	0.347	0.400	0.336	0.358
ϵ_b	0.003	0.006	0.010	0.0043	0.0055
$V/(V+PS)_{u,d}$	0.300	0.500	0.750	0.300	0.750
$V/(V+PS)_s$	0.250	0.600	0.750	0.500	0.750
$V/(V+PS)_{c,b}$	0.250	0.750	0.800	0.434	0.630
$\frac{s}{u}$	0.270	0.300	0.400	0.270	0.330
χ_d	0.094	0.164	0.226	0.118	0.180
χ_s	0.250	0.250	0.499	0.250	0.499
Baryon Fraction	0.080	0.100	0.120	0.080	0.120
Popcorn Parameter	0.000	0.500	2.000	0.000	2.000

Table 9: *Parameters, extremities and ranges used for the fragmentation tests of the correlation corrections.*

b-system are applicable. These event samples are then used to calculate the derivatives :

$$\Delta(\delta_b)_{syst.} = \sqrt{\sum_{i=1..}^{N_p} \frac{\partial^2 \left[(\sigma_{FB}^b)^2 - (\sigma_Q^b)^2\right]}{\partial^2 \mathrm{P}} \times Range^2} \qquad (12)$$

where N_p is the number of parameters and P represents the parameter in question. These derivatives (and their errors) are used, in conjunction with the ranges given in Table 9, to calculate the allowed variation of the correlation corrections for that parameter. The error on this *possible* degree of variation are also calculated. As these correlation corrections are calculated at the KINGAL, generator level, the variations are then scaled through to that expected at the simulated level. For example, at a κ of 0.5 the variations and errors are shown in Table 10. It is

Model Parameter	*Lower Range*	*Default*	*Upper Range*	$\Delta\delta_b$
λ_{QCD}	0.00880	0.00890	0.00872	0.00015
M_{min}	0.00875	0.00890	0.00885	0.00017
σ	0.00871	0.00890	0.00858	0.00022
ϵ_b	0.00851	0.00890	0.00848	0.00004
$V/(V+PS)_{u,d}$	0.00928	0.00890	0.00938	0.00017
$V/(V+PS)_s$	0.00948	0.00890	0.00930	0.00031
$V/(V+PS)_{c,b}$	0.00828	0.00890	0.00846	0.00032
$\frac{s}{u}$	0.00866	0.00890	0.00852	0.00024
χ_d	0.00901	0.00890	0.00900	0.00001
χ_s	0.00854	0.00890	0.00791	0.00112
Baryon Fraction	0.00882	0.00890	0.00882	0.00000
Popcorn Parameter	0.00907	0.00890	0.00928	0.00036

Table 10: *The effect of varying different fragmentation model parameters on the correlation corrections at $\kappa = 0.5$. The upper, lower and default values for the correlation corrections are given and the resulting uncertainty on the extraction of δ_b from $\bar{\delta}_b$.*

important to note that, within the KINGAL level Monte Carlo samples used, none of the above

devations are statistically significant. A conservative error estimate is obtained by adding all these *potential* error contributions in quadrature to form the systematic error on the correlation corrections.

For all values of κ the error from χ_s is dominant as its value is poorly known. It is likely that increased Monte Carlo statistics can significantly reduce this error to a similar level as that of other parameters.

5 Results

A summary of the extracted values of δ_b, with their statistical and systematic error contributions, is given in Table 11.

κ	δ_b	$\Delta(\delta_b)^{Data}_{Stat.}$	$\Delta(\delta_b)^{Life}_{Stat.}$	$\Delta(\delta_b)^{Life}_{Syst.}$	$\Delta(\delta_b)^{Corr}_{Syst.}$	$\Delta(\delta_b)_{Total}$
0.3	0.1102	0.0021	0.0033	0.0013	0.0007	0.0041
0.4	0.1258	0.0023	0.0030	0.0014	-	-
0.5	0.1413	0.0026	0.0029	0.0015	0.0013	0.0044
0.6	0.1570	0.0030	0.0030	0.0016	-	-
0.8	0.1863	0.0038	0.0034	0.0020	-	-
0.9	0.1996	0.0043	0.0035	0.0021	-	-
1.0	0.2126	0.0048	0.0038	0.0022	0.0042	0.0077
1.5	0.2615	0.0071	0.0047	0.0027	0.0078	0.0119
2.0	0.2909	0.0092	0.0053	0.0027	0.0106	0.0152
∞	0.3118	0.0259	0.0067	0.0023	-	-
		(a)	*(b)*	*(c)*	*(d)*	

Table 11: *Summary of results and error contributions to δ_b from $\bar{\delta}$. The errors are from : (a) the statistics of the data sample, (b) the Monte Carlo statistics used to make the lifetime dependent corrections, (c) the systematic error applied to the lifetime dependent corrections and (d) the systematic error from the correlation corrections.*

The systematic errors of Table 11 are not yet complete. It depends on two relatively small considerations :

- Updated correlation calculations in the KINGAL datasets for the remaining κ values omitted from Table 11.
- A cross-check that the systematic error on the lifetime-dependent corrections, derived from Figure 5 for κ=0.5, is sufficient for all values of κ.

This work is underway and updated estimates will be made available.

Substantial correlations exist between the measurements at different κ values, and hence between their statistical errors. The systematic errors are also correlated, but to varying degrees, depending on their source. As the measurements are made over a full range of quark flavours and statistical regimes, the separation of correlated and uncorrelated errors as a function of κ is not straightforward.

6 Acknowledgements

The authors would like to thank Alain Blondel, Dave Brown, Rick St. Denis and Pascal Perrodo for their help, numbers and useful discussions.

7 Appendix : Extraction of δ_b from $\bar{\delta}_b$

If we assume for the moment that only one type of quark flavour ($f\bar{f}$) is present, then it is possible to separate hadronic events into two types :

(a) Events with the *quark* moving in the forward direction with their associated quantities : $Q^f_{FB}, \sigma^f_{FB}, Q^f, \sigma^f_Q$ etc. and

(b) Events with the *antiquark* moving in the forward direction with their associated quantities : $Q^{\bar{f}}_{FB}, \sigma^{\bar{f}}_{FB}, Q^{\bar{f}}, \sigma^{\bar{f}}_Q$ etc.

The quark-forward and antiquark-forward distributions are conjugates of each other, so that their means and widths are equal in absolute magnitude :

$$\begin{aligned} \langle Q^f_{FB} \rangle \equiv \delta_f = -\delta_{\bar{f}} \equiv -\langle Q^{\bar{f}}_{FB} \rangle \quad \text{and} \quad \sigma^f_{FB} = \sigma^{\bar{f}}_{FB} \\ \langle Q^f \rangle = \langle Q^{\bar{f}} \rangle \quad \text{and} \quad \sigma^f_Q = \sigma^{\bar{f}}_Q \text{ etc.} \end{aligned} \tag{13}$$

In data, both quark and antiquark-forward configurations are present so that measurements are made of :

$$\sigma^{f\bar{f}}_{FB} = \sqrt{Var\, Q_{FB}} = \sqrt{Var\,(Q_F - Q_B)} \tag{14}$$

$$\sigma^{f\bar{f}}_Q = \sqrt{Var\, Q} = \sqrt{Var\,(Q_F + Q_B)} \tag{15}$$

The relation between $\bar{\delta}_f$ and the hemisphere-charge separation, δ_f, may be written more explicitly as :

$$\bar{\delta_f}^2 = \frac{N_f}{N_f + N_{\bar{f}}} \langle \left(Q^f_{FB}\right)^2 - \left(Q^f\right)^2 \rangle + \frac{N_{\bar{f}}}{N_f + N_{\bar{f}}} \langle \left(Q^{\bar{f}}_{FB}\right)^2 - \left(Q^{\bar{f}}\right)^2 \rangle - \langle Q^{f\bar{f}}_{FB} \rangle^2 + \langle Q^{f\bar{f}} \rangle^2 \tag{16}$$

where N_f and $N_{\bar{f}}$ are the numbers of quark and antiquark-forward configurations respectively. The $f\bar{f}$ superscript refers to the (typical) situation where both quark and antiquark-forward cinfigurations are present in the sample. If we consider only one configuration for a moment, then we can write :

$$\begin{aligned} \left(\sigma^f_{FB}\right)^2 &= \langle \left(Q^f_{FB}\right)^2 \rangle - \langle Q^f_{FB} \rangle^2 \\ &= \langle \left(Q^f_{FB}\right)^2 \rangle - \delta_f^2 \end{aligned} \tag{17}$$

Similarly for the total charge distribution :

$$\langle \left(Q^f\right)^2 \rangle = \langle Q^f \rangle^2 + \left(\sigma^f_Q\right)^2 \tag{18}$$

Inserting relations (17) and (18) into equation (16) yields :

$$\bar{\delta_f}^2 = \frac{N_f}{N_f + N_{\bar{f}}} \delta_f + \frac{N_{\bar{f}}}{N_f + N_{\bar{f}}} \delta_{\bar{f}} - \langle Q^{f\bar{f}}_{FB} \rangle^2 + \left(\sigma^f_{FB}\right)^2 - \left(\sigma^f_Q\right)^2 \tag{19}$$

The term, $\langle Q^{f\bar{f}}_{FB} \rangle^2$, represents the actual electroweak asymmetry itself and is taken directly from data measurements.

The correction from Monte Carlo, which must be applied to $\bar{\delta}_b$ to obtain δ_b, represents the correlation between measurements of the weighted charge in each hemisphere. This is apparent from :

$$\begin{aligned} \left(\sigma^b_{FB}\right)^2 - \left(\sigma^b_Q\right)^2 &= \left(\sigma^b_F\right)^2 + \left(\sigma^b_B\right)^2 - 2\,Cov\left(Q^b_F, Q^b_B\right) - \\ &\quad \left(\sigma^b_F\right)^2 - \left(\sigma^b_B\right)^2 - 2\,Cov\left(Q^b_F, Q^b_B\right) \\ &= -4\left[\langle Q^b_F Q^b_B \rangle - \langle Q^b_F \rangle \langle Q^b_B \rangle\right] \end{aligned} \tag{20}$$

which is simply the 4 × correlation between the measurements of the quark and antiquark hemisphere charges in each half of the events. The main sources of correlation are expected to arise from the determination of a common thrust axis and the "cross-over" of soft particles close to the hemisphere boundary. These in turn will depend on the power, κ, which is applied during the weighted charge summation. The sources of correlation are well modelled in simulated events and are unlikely to be strongly dependent on fragmentation.

References

[1] D. Decamp et al. (The ALEPH Collaboration), *"Measurement of Charge Asymmetry in Hadronic Z Decays"*, Physics Letters B 259 (1991) 377.

[2] P. Abreu et al. (The DELPHI Collaboration), *"A Measurement of $sin^2\theta_W$ from the Charge Asymmetry of Hadronic Events at the Z^0 Peak"*, Physics Letters B 277 (1992) 371.

[3] P.D. Acton et al. (The OPAL Collaboration), *" A Measurement of the Forward-Backward Charge Asymmetry in Hadronic Decays of the Z^0"*, Physics Letters B 294 (1992) 436.

[4] D. Buskulic et al. (The ALEPH Collaboration), *"Measurement of $B^0 - \bar{B}^0$ Mixing at the Z using a Jet-Charge Method"*, Physics Letters B 284 (1992) 177.

[5] A. Blondel et al. *"Determination of $sin^2\theta_w^{eff}$ From the Hadronic Charge Asymmetry"*, ALEPH Note 93-33, PHYSIC 93-35.

[6] A. Halley (The ALEPH Collaboration), Presentation to the International Europhysics Conference on High Energy Particle Physics, Marseilles, France, 22-28 July 1993.

[7] I. ten Have, *An Updated Measurement of the b Charge Separation in a Lepton-tagged Sample*, ALEPH Note 93-141 PHYSIC 93-121.

[8] A. Halley and P. Colrain, *A Preliminary Measurement of $sin^2\theta_w^{eff}$ from $A_{FB}^{b\bar{b}}$ in the 1992 Lifetime-Tagged Heavy-Flavour Sample*, ALEPH Note 93-134, PHYSIC 93-115

[9] D. Brown and M. Frank, *"Tagging b Hadrons Using Track Impact Parameters"*, ALEPH Note 92-135, PHYSIC 92-124.

[10] D. Buskulic et al. (The ALEPH Collaboration), *"A Measurement of $\Gamma_{b\bar{b}}/\Gamma_{had}$ Using a Lifetime b-Tag"*, CERN Preprint PPE 93-108.